Remodeling of the infection chamber before infection thread formation reveals a two-step mechanism for rhizobial entry into the host legume root hair

Plant Physiology Preview. Published on February 6, 2015, as DOI:10.1104/pp.114.253302

Running head : **Rhizobial infection chamber remodeling**

Corresponding author : Joëlle Fournier
Laboratoire des Interactions Plantes Micro-organismes, Institut National de la Recherche Agronomique (UMR 441), Centre National de la Recherche Scientifique (UMR 2594), F-31320 Castanet-Tolosan, France.

Telephone: +33 561 285 508
Email: joelle.fournier@toulouse.inra.fr

Research area: **Cell Biology**

Remodeling of the infection chamber prior to infection thread formation reveals a two-step mechanism for rhizobial entry into the host legume root hair.

Joëlle Fournier[1], Alice Teillet[1], Mireille Chabaud[1], Sergey Ivanov[2], Andrea Genre[3], Erik Limpens[2], Fernanda de Carvalho-Niebel[1] and David G. Barker[1]

[1]Laboratoire des Interactions Plantes Micro-organismes, Institut National de la Recherche Agronomique (UMR 441), Centre National de la Recherche Scientifique (UMR 2594), F-31320 Castanet-Tolosan, France.

[2] Plant Science - Laboratory of Molecular Biology, Wageningen University, Wageningen, 6708PB, The Netherlands.

[3] Dipartimento di Scienze della Vita e Biologia dei Sistemi, Università di Torino, 10125 Torino, Italy.

One-sentence summary:

Legume root hairs remodel the interface with symbiotic rhizobia prior to initiating the tubular-growing infection thread.

Footnotes:

This work was supported in part by a French National Research Agency grant to D.G.B. (reference ANR-08-BLAN-0029-01), a PHC Galilée 2014 grant to A.G. and D.G.B. (reference 30111WJ) and a French Ministry of Education and Research fellowship to A.T. This study is part of the French National Laboratoire d'Excellence (LABEX) initiative entitled TULIP (grant no. ANR-10-LABX-41).

Present address for Alice Teillet is: Department of Plant Pathology, University of Wisconsin-Madison, Madison, Wisconsin 53706-1598, United States of America

Present address for Sergey Ivanov is: Boyce Thompson Institute for Plant Research, Ithaca, New York 14853-1801, United States of America

Corresponding author : Joëlle Fournier
email: joelle.fournier@toulouse.inra.fr

Abstract

In many legumes, root entry of symbiotic nitrogen-fixing rhizobia occurs *via* host-constructed tubular tip-growing structures known as infection threads. Here we have used a confocal microscopy live-tissue imaging approach to investigate early stages of infection thread formation in *Medicago truncatula* root hairs expressing fluorescent protein fusion reporters. This has revealed that infection threads only initiate 10-20 h after the completion of root hair curling, by which time major modifications have occurred within the so-called infection chamber, the site of bacterial entrapment. These include the accumulation of exocytosis (MtVAMP721e) and cell wall (MtENOD11)-associated markers, concomitant with radial expansion of the chamber. Significantly, the infection-defective *Mtnin-1* mutant is unable to create a functional infection chamber. This underlines the importance of the *NIN*-dependent phase of remodeling of the host cell wall that accompanies bacterial proliferation and precedes infection thread formation and leads us to propose a novel two-step model for *Rhizobium* infection initiation in legume root hairs.

Introduction

Legumes possess the remarkable capacity to improve their nutrition by establishing a nitrogen-fixing root nodule symbiosis (RNS) with soil bacteria collectively called rhizobia. In many legumes such as *M. truncatula,* rhizobia penetrate across the root epidermis and outer cortex to reach the differentiating nodule tissues *via* sequentially constructed transcellular compartments known as infection threads (ITs; Gage, 2004). It is now well established that this mode of entry through specialized infection compartments, often referred to as accommodation, is shared with the more ancient arbuscular mycorrhizal (AM) symbiosis from which the legume-*Rhizobium* RNS is thought to have evolved (Parniske, 2008; Markmann and Parniske, 2009). Furthermore, strong evidence indicates that the signaling and cellular mechanisms underlying IT formation in legumes are closely related to those used for infection compartment formation during AM infection of epidermal and outer cortical tissues (Bapaume and Reinhardt, 2012; Oldroyd, 2013).

Rhizobial infection is set in motion after an initial molecular dialogue between symbiotic partners, in which rhizobial lipochito-oligosaccharide Nod factors (NFs) are key signaling molecules (reviewed in Oldroyd, 2013). Host responses to NF signaling include rapid and sustained nuclear-associated Ca^{2+} oscillations (Ca^{2+} spiking) (Ehrhardt et al., 1996; Oldroyd and Downie, 2006; Sieberer et al., 2009; Capoen et al., 2011) and the rapid expression of early epidermal marker genes such as *M. truncatula ENOD11* (Charron et al., 2004). The activation of nuclear Ca^{2+} spiking is one of the most characteristic features of the so-called SYM signaling pathway, common to both RNS and AM (Kistner and Parniske, 2002; Singh and Parniske, 2012). Whilst these pre-infection responses to NFs are observed in the majority of elongating root hairs (RHs) early after rhizobial inoculation (Journet et al., 2001; Wais et al., 2002), ITs are only formed in a small sub-set of RHs, and *MtENOD11* expression is strongly activated at these rhizobial infection sites (Journet et al., 2001; Boisson-Dernier et al., 2005).

ITs are tubular plant-derived structures delimited by a membrane which is contiguous with the RH plasmalemma and a layer of cell wall-like material, thus isolating the rhizobia from the host cell cytoplasm (Gage, 2004). These apoplastic infection compartments are progressively constructed along the length of the RH with their growing tip connected *via* a cytoplasmic bridge to the migrating RH nucleus. This broad cytoplasmic column provides the cell machinery for tip growth which involves targeted exocytosis of membrane and extracellular materials to the growing apex of the IT (Oldroyd et al., 2011; Bapaume and Reinhardt, 2012). It is presumed that this cytoplasmic bridge shares an equivalent role to the pre-penetration apparatus (PPA) formed at the onset of AM fungal infection (Genre et al., 2005; Genre et al., 2008). We now know that the IT tip region is formed in advance of rhizobial colonization and is progressively populated by dividing rhizobia which also

physically move down the thread (Gage, 2004; Fournier et al., 2008). It has been proposed that the matrix of the growing IT tip is initially in a fluid or gel-like state compatible with bacterial growth and movement (Brewin, 2004; Fournier et al., 2008). This relative plasticity could result in part from the presence of atypical extracellular (glyco)-proteins such as the repetitive Pro-rich proteins MtENOD11/12 because their low Tyr content is presumed to limit cross-linking to other wall components (Scheres et al., 1990; Pichon et al., 1992; Journet et al., 2001).

Nevertheless, the mechanism by which rhizobial IT formation is initiated in RHs is not clear. Whereas AM fungal hyphae form contact structures called hyphopodia on the exposed surface of non-hair epidermal cells prior to PPA formation and peri-fungal infection compartment formation (Genre et al., 2005), rhizobial entry requires that the bacteria first become entrapped between RH walls. Attachment of rhizobia close to a growing RH tip induces a continuous reorientation of tip growth, most likely the result of localized NF production (Esseling et al., 2003), eventually leading to RH curling and subsequent bacterial entrapment within a closed chamber in the centre of the curl (Catoira et al., 2001; Geurts et al., 2005). Rhizobial entrapment can also occur between the cell walls of two touching RHs (Dart, 1974; Gage, 2004).

The closed chamber in curled RHs has often been termed the infection pocket (e.g. Murray, 2011; Guan et al., 2013). However, because this term is also used to designate a quite different and larger structure formed in root sub-epidermal tissues of legumes during intercellular infection following “crack entry” and involving localized cell death (Goormachtig et al., 2004), we propose to use the term “infection chamber” to describe the unique enclosure formed during rhizobial RH infection.

Following entrapment, it has been proposed that rhizobia multiply to form a so-called ‘microcolony’ (Gage et al., 1996; Limpens et al., 2003) and that IT polar growth initiates in front of this microcolony by local invagination of the RH plasmalemma combined with exocytosis of extracellular materials (Gage, 2004). Furthermore, it has been suggested that localized degradation of the chamber wall would allow the rhizobia to access the newly formed IT (Callaham and Torrey, 1981; Turgeon and Bauer, 1985). However a detailed investigation of this particular stage of rhizobial infection is missing and in particular when and where the rhizobia/cell wall interface becomes modified. Such studies have been limited until now, notably because ITs develop only in a low proportion of curled RHs (Dart, 1974).

To attempt to answer this question we have used a live tissue imaging approach developed for in vivo confocal microscopy in *M. truncatula* (Fournier et al., 2008; Cerri et al., 2012; Sieberer et al., 2012), and particularly well adapted to time-lapse studies of the initial stages of rhizobial infection including RH curling and IT formation. To investigate modifications occurring at the RH interface with the enclosed rhizobia during these early stages, we

prepared *M. truncatula* plants expressing fluorescent protein fusions aimed to detect both exocytosis activity and cell wall remodeling during the initial construction of the IT apoplastic compartment. To this end we made use of the *M. truncatula* Vesicle-Associated Membrane Protein721e (MtVAMP721e; Ivanov et al., 2012) recently shown to label exocytosis sites in both growing RHs and during AM colonization (Genre et al., 2012) as well as the infection and cell-wall associated MtENOD11 Pro-rich glycoprotein (Journet et al., 2001). Our experiments have revealed that IT development in curled RHs only initiates after a lengthy interval of 10-20 h during which sustained exocytosis and MtENOD11 secretion to the infection chamber is associated with radial expansion as well as remodeling of the surrounding walls. Importantly, it was found that the infection-defective *Mtnin-1* mutant (Marsh et al., 2007) is impaired in chamber remodeling. Our findings lead us to propose a new model for IT formation in which the infection chamber first differentiates into a globular apoplastic compartment displaying similarities to the future IT and in which the enclosed rhizobia multiply. This is then followed by a switch from radial to tubular growth corresponding to tip-driven IT growth and associated movement of rhizobia into the extending thread. Importantly, this two-step model no longer requires that the host cell wall is degraded in order to allow access of the colonizing rhizobia to the newly initiated IT.

Results

Infection thread tip-growth in M. truncatula initiates 10-20 hours after the completion of root hair curling

In order to study the cellular events associated with IT initiation, a live-tissue imaging approach was used to identify and continuously monitor RHs at different stages of curling and rhizobial entrapment (Fournier et al., 2008; Cerri et al., 2012). The observation of many such RHs surprisingly revealed that IT tip growth only initiated many hours following the completion of curling and in no case did we observe IT formation immediately after curling. In the example shown in Fig. 1, RH curling around the entrapped rhizobia is close to completion at the initial time point of observation (Fig. 1A). The unchanged position of the RH tip in Fig. 1B-C (single arrowhead) indicates that curling had terminated during the first 1.5 h period. Tubular IT formation was not observed during the following 7.5 h despite the fact that the nucleus and associated cytoplasm are stably localized in the curled tip region of the RH (Fig. 1B-D). However, a growing IT was observed within this particular RH 15 h later (Fig. 1E) and continued its progression during the following hours (not shown). Based on the length of the IT in Fig. 1E, we estimate that elongation had been underway for approximately 6-8 h (average growth rate of ITs is 4-5 $\mu m.h^{-1}$ in *M. truncatula*; Fournier et al., 2008). Thus, in this particular case, the delay between the completion of RH curling and IT initiation can be

estimated to be around 15-18 h. Similar image series obtained for a number of other RHs initiating infection have together revealed that the delay between the completion of bacterial entrapment and IT initiation is in the range of 10-20 h. During this lengthy period the infection chamber became progressively easier to distinguish from the surrounding cytoplasm, most likely as a consequence of enlargement and surface modifications prior to IT initiation (Suppl. Fig. S1). To further investigate this, we have exploited fluorescent cellular markers for monitoring both host exocytosis activity and possible modifications to the infection chamber extracellular matrix.

The GFP-MtVAMP721e exocytosis marker accumulates rapidly around the newly formed infection chamber

To evaluate potential exocytosis activity associated with the RH infection chamber we made use of *M. truncatula* plants expressing a fluorescence-tagged MtVAMP721e (Genre et al., 2012; Ivanov et al., 2012) in their roots. In non-inoculated or non-colonized RHs, the GFP-MtVAMP721e fusion protein primarily localizes to the vesicle-rich region behind the growing tip of elongating RHs and at lower levels as localized puncta elsewhere in the cytoplasm (Genre et al., 2012, and Fig. 2A). Our *in vivo* observations have revealed that the GFP-VAMP721e fluorescent signal is no longer located to the RH tip region of fully curled RHs with entrapped rhizobia, but now surrounds the infection chamber, outlining its contours (Fig. 2A). This signal is presumably associated with the plasma membrane bordering the infection chamber, most likely corresponding to the accumulation of GFP-VAMP-labeled vesicles. By monitoring such curled RHs over time, we further discovered that the exocytosis reporter is continuously present around the infection chamber (e.g. over the entire 7 h period illustrated in Fig.2A-C). This suggests a lengthy period of sustained exocytosis targeted towards the infection chamber. This continuous exocytosis activity was directly associated with radial expansion of the infection chamber at the same period of time. Our results thus argue that membrane and extracellular material are actively conveyed towards the infection chamber following the completion of RH curling and prior to IT initiation. As illustrated in Fig. 2D-F, the continuous enlargement of the infection chamber is accompanied by progressive multiplication of the enclosed rhizobia.

In order to investigate in more detail when host membrane/cell wall interface remodeling is initiated following RH curling, we focused on the earliest stages of infection chamber formation. Tip-focused accumulation of GFP-MtVAMP721e characteristic of elongating RHs (Genre et al., 2012, and Fig. 2A) persists during RH curling around attached rhizobia (Fig. 2G and I). However, as soon as RH tip curling is completed fluorescence labeling at the RH tip is lost (Fig. 2H, dashed arrow). Importantly, Figure 2J shows that the accumulation of

GFP-MtVAMP721e around enclosed rhizobia initiates within the first hours following the completion of RH tip curling. Taking into account the fact that rhizobial cell division within growing *Medicago* ITs takes at least 4h (Gage, 2002), these findings imply that exocytosis of extracellular material towards the newly formed infection chamber initiates before significant rhizobial multiplication has occurred within the chamber.

The Mtnin-1 *mutant is impaired for exocytosis targeted to the infection chamber*

We next investigated whether exocytosis targeted to the infection chamber occurred in the case of the infection mutant *Mtnin-1,* which is able to enclose rhizobia by RH curling but fails to form ITs and shows impaired multiplication of the enclosed rhizobia (Marsh et al., 2007; Murray, 2011). Indeed, compared to wild type plants where large rhizobial microcolonies were present within curled RHs (Fig. 3A), few bacteria were detectable within curled RHs in the *Mtnin-1* mutant (Fig. 3B-C and Fig. 3D-F). Monitoring GFP-VAMP721e fusion exocytosis-related localization in *nin* RH curls revealed that in this case the entrapment of rhizobia in curled RHs was never followed by GFP-VAMP721e accumulation around the infection chamber (Fig. 3D-F and Suppl. Fig. S2), despite the fact that the localization of the fusion protein at the tip of growing RHs was otherwise similar to that in wild type (Suppl. Fig. S3). Furthermore, the nucleus and associated cytoplasm moved down the RH shaft after a few hours in the *nin* mutant (Fig.3 D-F) whereas they remain close to the enclosed bacteria in wild type plants (Fig.1 A-D, Fig. 2A-C). The absence of exocytotic activity is consistent with the lack of radial expansion of the infection chamber in curled *nin* RHs (Fig. 3G-I and Suppl. Fig. S2). Taken together, this indicates that MtNIN is required to initiate the remodeling of the infection chamber following rhizobial entrapment.

The extracellular MtENOD11 protein is targeted to the infection chamber following rhizobial entrapment

To examine whether exocytotic activity in the infection chamber is associated with cell wall remodeling, we monitored the accumulation of the rhizobial infection-associated extracellular protein MtENOD11. Recently we have found that a YFP-tagged MtENOD11 fusion protein, when expressed under the control of native promoter sequences (Boisson-Dernier et al., 2005), accumulates at the periphery of elongating ITs in *M. truncatula* RHs, and especially at the growing IT tips (Fournier, Teillet, Auriac, Barker, de Carvalho-Niebel, manuscript in preparation). Using the same YFP-tagged protein fusion, an intense fluorescent signal could be observed within the center of the curled hair before IT formation (Fig. 4A-B). This focalized accumulation around the entrapped bacteria is similarly observed in the less

frequent situation where the symbiotic bacteria have become entrapped between the walls of two growing RHs (Fig. 4C-D). Once the tubular IT has initiated from the infection chamber, the fluorescent protein is also found associated to the growing IT tip as expected (Fig. 4C). The intense YFP-MtENOD11 fluorescence is specific to the cell wall matrix associated with rhizobial infection structures including the infection chamber, contrasting with the very low levels of YFP fluorescence labeling the RH walls (Fig. 4A-B and Fournier, Teillet, Auriac, Barker, de Carvalho-Niebel, manuscript in preparation). This implies that the cell wall matrix surrounding rhizobia has a particular composition that is distinct from the normal RH extracellular matrix. In line with this, this region also differs with respect to cell wall auto-fluorescence. RH walls display intrinsic fluorescence that can be used to visualize the cell contours (e.g. Fig. 1A-E, right panels and Fig. 4B). Under identical conditions, the wall matrix directly surrounding the enclosed rhizobia and corresponding to the region of maximal YFP-MtENOD11 accumulation (Fig. 4A) is totally devoid of auto-fluorescent material (Fig. 1A-E and Fig. 4B). Intriguingly, a strong auto-fluorescent signal can be observed in a limited region of the wall adjacent to the infection chamber (Fig. 1C-E and Fig. 4B). Additional studies will be needed to identify the chemical nature of this autofluorescent material, whose accumulation is independent of exocytosis processes related to MtVAMP721e, and whether it results from local increased secretion of phenolics or other compounds, or from enzymatic modifications to existing cell wall components. In conclusion, these observations indicate that during the lengthy period between RH curling and IT initiation, the wall/matrix surrounding the rhizobia within the expanding infection chamber is characterized by the absence of auto-fluorescent material and a strong and focused accumulation of the MtENOD11 Pro-rich protein, supporting the idea that specific wall remodeling is taking place in the chamber during this period.

Discussion

During the establishment of the RNS in many legumes such as *M. truncatula* root entry by rhizobia occurs *via* a process which initiates with the physical entrapment of the bacteria between RH cell walls followed by the formation of the tip-growing apoplastic ITs. In order to initiate studies on the molecular/cellular processes which accompany the transition between rhizobial entrapment and IT formation we performed time-lapse confocal imaging on *M. truncatula* roots undergoing rhizobial colonization. These experiments unexpectedly revealed that there is a lengthy delay (from 10-20 h) before tubular IT formation is initiated from within fully curled RHs (Fig. 1). Although rarely examined in earlier studies of rhizobial infection, this finding is consistent with light microscopy experiments performed over 30 years ago on inoculated clover roots (Callaham and Torrey, 1981). Most importantly, our live-tissue

imaging studies provide strong evidence that major, *NIN*-dependent host cell wall re-modeling occurs within the infection chamber throughout the entire period preceding IT initiation, and this discovery leads us to propose a new two-stage model to explain the cellular mechanisms underlying this critical phase of rhizobial RH infection.

Remodeling of the infection chamber into a novel infection thread-like compartment

The localization of fluorescent markers labeling both the exocytosis reporter MtVAMP721e and the infection-associated secreted protein MtENOD11 have shown that the RH cell actively remodels the infection chamber during the 10-20 h period preceding IT formation (Fig. 2 and Fig. 4). Indeed, this sustained exocytotic activity and concomitant deposition of extracellular material visualized with the MtENOD11 fusion protein correlates with progressive enlargement of the infection chamber (Fig.2 and Suppl. Fig. S1), a stage that has been described as the development of the 'refractile spot' or 'cell wall swelling' in early studies (Fåhraeus, 1957).

Although the early accumulation of MtENOD11 throughout the period of infection chamber remodeling is consistent with the early transcriptional activation of the gene in curled RHs before IT formation (Boisson-Dernier et al., 2005), the focalized accumulation of the MtENOD11 protein exclusively around the entrapped bacteria is an intriguing observation. The Pro-rich MtENOD11 is an atypical cell wall-associated protein with unusually low Tyr content, presumed to limit cross-linking to other wall components (Journet et al., 2001). As such, the accumulation of MtENOD11 within the chamber is likely to contribute to the cell wall plasticity required for the radial expansion and the subsequent polar initiation of ITs. The occurrence of MtENOD11 within the infection chamber therefore leads us to propose a scenario in which the chamber progressively acquires an IT-like composition prior to tip-growth initiation (Fig. 5 and Suppl. Movie1). In this scenario, the transport of exocytotic vesicles towards the membrane surrounding the infection chamber initiates within hours following the completion of RH curling (Fig. 5A-D). Progressive deposition of new membrane and extracellular materials including MtENOD11 over the following 10-20 h leads to radial infection chamber enlargement and conversion into a globular IT-like compartment (Fig. 5E and Suppl. Movie1). This is accompanied by a small number of rhizobial cell divisions (see below). At the end of this first phase a switch from radial expansion to polar tip elongation leads to the initiation of IT development (Fig. 5F and Suppl. Movie1). In this two-step model, the *Mtnin-1* mutant fails to initiate the first stage of infection chamber remodeling (corresponding to the transition between stages C and D shown in Fig. 5). In conclusion, we therefore propose that IT initiation should be viewed as a tip-growing extension emanating from the IT-like compartment already created within the infection chamber. One important consequence of this model is that there is no longer any need to hypothesize that localized

host cell wall degradation is required for colonizing rhizobia to access the newly formed IT in contrast to what was previously proposed (Callaham and Torrey, 1981; Turgeon and Bauer, 1985; Gage, 2004). Finally, it should be underlined that our findings also clearly argue against an additional suggestion that the initiation of IT development might result from a direct conversion of apical RH tip-growth to inward-directed IT tip-growth (e.g. Brewin, 1991; Kijne, 1992).

Plant-microsymbiont signal exchange during the two stages of rhizobial entry

In the light of this new two-step model for rhizobial infection, what do we know about the various factors that are involved in infection chamber remodeling and the initiation of tubular IT growth? Recent data has revealed that *Rhizobium*-elicited Ca^{2+} spiking in the RH is strongly attenuated in fully curled hairs with entrapped rhizobia, and that sustained spiking is re-activated prior to and during the entry of the bacteria into the newly created IT (Sieberer et al., 2015). This suggests that there are sequential modifications in the host perception of rhizobial LCO signals during these key stages, and that the capacity to perceive these signals may be important in the triggering of IT initiation. Indeed, this is in line with the proposal that IT development within the *M. truncatula* RH requires that the host perceives NF-related signals *via* a specific "entry" receptor involving the LysM receptor-like kinase LYK3 (Limpens et al., 2003; Smit et al., 2007). Further evidence for distinct sequential steps prior to IT formation comes from the *S. meliloti nodFnodL* mutant which produces abnormal NFs and cannot activate IT formation, despite the fact that rhizobial entrapment and multiplication take place (Ardourel et al., 1994) in addition to the trigger of infection-related *MtENOD11* expression (Boisson-Dernier et al., 2005). Confocal imaging experiments have revealed that a single attached bacterium is often sufficient to induce initial RH tip curling (Fig. 1, Fig. 2G, H) and that a small rhizobial micro-colony comprising from 10-30 bacteria is present within the infection chamber by the time the IT is initiated (Fig. 2 D-F). It is conceivable that rhizobial multiplication within the chamber may be an important parameter in generating threshold levels of bacterial signal molecules required for triggering IT initiation. Furthermore, the modified environment generated within the chamber by focused exocytosis may play a role in activating rhizobial differentiation and associated responses necessary for successful infection including the secretion of infection-related LCOs and other important components such as acidic exopolysaccharides (reviewed in Downie, 2010).

The *nin* mutants in *Lotus,* pea or *M. truncatula* (Schauser et al., 1999; Borisov et al., 2003; Marsh et al., 2007) are able to respond to rhizobial inoculation by RH curling leading to rhizobial entrapment (a stage depicted in Fig. 5C) but do not progress to tubular IT initiation. We now show that this is most likely the result of the failure of infection chamber remodeling and associated microcolony development. In *Lotus,* the recently characterized pectate lyase

NPL (Xie et al., 2012) that is required for proper infection is regulated by NIN. It is therefore possible that the infection-defective phenotype of *Mtnin*-1 results at least in part from the lack of expression of an orthologous *M. truncatula* pectate lyase. Identifying and characterizing NIN targets in *Medicago* will be important to understand the infection chamber remodeling process. The two-step model for infection is also consistent with the phenotypes of other legume mutants defective for rhizobial infection. For example, *Ljcyclops* (Yano et al., 2008) or *Mtlin* (Kuppusamy et al., 2004; Guan et al., 2013) mutants appear to be impaired at the intermediate stage (depicted in Fig. 5E) following rhizobial microcolony development but preceding tubular IT initiation. It will now be important to identify and study additional host and bacterial cell wall-associated components involved in the development of the rhizobial infection chamber compartment including cell wall modifying enzymes proposed to be required for IT formation such as *Lotus* NPL (Xie et al., 2012) or the *Rhizobium* cell-bound cellulase CelC2 (Robledo et al., 2008).

Is infection chamber remodeling a specificity of the Rhizobium-legume symbiosis?

As underlined in the introduction, there are a number of striking similarities between the early infection stages of the rhizobial and AM associations, both in terms of host/microbe signaling pathways and the mechanisms involved in the respective host-regulated apoplastic infection processes (Parniske, 2008; Bapaume and Reinhardt, 2012). AM fungi also penetrate plant roots via a host-constructed transcellular compartment equivalent to the rhizobial IT. The development of this specialized peri-fungal compartment is prefigured by the formation of the transient cytoplasmic PPA, which links the migrating cell nucleus to the site of AM fungal attachment via the hyphopodium (Genre et al., 2005; Genre et al., 2008). In addition, Rich *et al.* (2014) have recently proposed that host cell-driven modifications to the cell wall at the site of hyphopodium contact would precede *Rhizophagus irregularis* entry into the *Petunia hybrid* root. Thus, by analogy with the creation of the IT precursor within the enclosed space formed by RH curling, it is possible that hyphopodium attachment also creates an enclosed environment within which host secretion and associated wall remodeling generates a specialized compartment, thus allowing the AM hyphae to cross the host cell wall. Future studies focused on this key step preceding AM fungal cell penetration will now be needed to address this intriguing question.

Materials and Methods

Biological materials

The *M. truncatula sunn-2* mutant was used for most of the experiments described in this article because its enhanced infection phenotype (Schnabel et al., 2005) greatly facilitates the identification of RH infection sites, whilst at the same time possessing a normal wild type infection process (Fournier et al., 2008; Cerri et al., 2012; Sieberer et al., 2012). The *M. truncatula nin-1* mutant, kindly provided by Giles Oldroyd and Tatiana Vernié, and *M. truncatula* cv Jemalong A17 were also used in this study, and all plants were grown as described previously (Fournier et al., 2008). Strains of *Sinorhizobium meliloti* 2011 constitutively expressing either GFP (*Sm* 2011-GFP) or the Cerulean version of CFP (*Sm* 2011-cCFP) (both kindly provided by P. Smit, University of Wageningen, The Netherlands) or a *hemA-lacZ* fusion (*Sm* 2011-*lacZ*; Ardourel et al., 1994) were propagated as described (Cerri et al., 2012).

Expression of fluorescent protein fusions in M. truncatula roots

The GFP-MtVAMP721e fusion (Ivanov et al., 2012) was expressed under the control of the *A. thaliana UBQ3* promoter in a pK7WGF2-R-derived binary vector carrying the 'Red Root' selection marker which comprises the DsRed coding sequence driven by the *A. thaliana UBQ10* promoter (Smit et al., 2005; Limpens et al., 2009). The construction of the chimeric gene expressing YFP-labelled MtENOD11 is described in detail in (Fournier, Teillet, Auriac, Barker, de Carvalho-Niebel, in preparation). In this construct YFP has been inserted between the N-terminal ENOD11 signal peptide (75 bp) and the remaining repetitive Pro-rich domain (450 bp), and expression is driven by a 1 kb fragment of the endogenous ENOD11 promoter (pE11) that is sufficient for both pre-infection and infection-related expression (Boisson-Dernier et al., 2005). The pUBQ3-GFP-MtVAMP721e and pE11-YFP-MtENOD11 constructs were introduced into *Agrobacterium rhizogenes* ARqual (Quandt et al., 1993) and composite *sunn*-2 or *nin-1* plants were produced *via A. rhizogenes*-mediated transformation as described in (Boisson-Dernier et al., 2001). Composite plants with roots constitutively expressing the GFP-MtVAMP721e fusion were selected under the stereomicroscope for moderate and uniform fluorescence levels. Those with roots expressing pE11-YFP-MtENOD11 were selected on Fåhraeus medium supplemented with 25 $\mu g.ml^{-1}$ kanamycin.

In vivo microscopy of rhizobial infection sites in root hairs

Rhizobial inoculation for *in vivo* microscopic observation was performed essentially as described (Fournier et al., 2008; Sieberer et al., 2012). Briefly, plants were placed in 12x12cm Petri dishes containing a modified Fåhraeus medium (Phytagel 0.5%) supplemented with 50nM 2-amino ethoxyvinyl glycine (AVG). Roots were covered with a

gas-permeable plastic film (Lumox Film, Starsted, France), and plants grown with the dishes slightly tilted to encourage the growth of the roots along the plastic film. Inoculation with *Sm* 2011-GFP or *Sm* 2011-cCFP strains was performed by introducing 0.5-1 mL of an aqueous suspension of exponentially growing bacteria (OD_{600} = 0.001; approx. 10^6 bacteria.mL^{-1}) under the plastic film. To investigate the early stages of rhizobial infection, roots of inoculated plants were observed 1 to 4 d post-inoculation. Curled RHs with enclosed fluorescent bacteria as well as bacterial entrapment between cell walls of adjacent RHs were identified as potential sites for imaging. In addition, preference was given to curled RHs where the nucleus was located close to the enclosed rhizobia and associated with significant quantities of cytoplasm since experience had shown that these were more likely to initiate ITs. Plants were returned to the culture room between observations. Data were obtained from a total of 18 experiments in *sunn-2* and 2 experiments in Jemalong A17 and *Mtnin-1*. The results presented are representative of observations recorded on 27 (Fig. 1), 24 (Fig. 2), 10 (Fig. 3D-I) and 15 (Fig. 4) rhizobial infection sites, monitored using 20, 15, 2 and 12 independent plants, respectively. The duration of the interval between curl closure and IT initiation was evaluated for 7 sites (5 independent experiments) and corroborated by data from an additional 20 sites monitored over longer intervals.

Confocal microscopy

Selected infection sites were imaged with a Leica TCS SP2 AOBS confocal laser scanning microscope equipped with a long-distance 40x HCX Apo L NA 0.80 water-immersion objective. The argon laser bands of 458nm, 488nm and 514nm were used to excite CFP, GFP and YFP, respectively, and a 561-nm diode to excite the DsRed and observe cell wall autofluorescence. Specific emission windows used for CFP, GFP, YFP, DsRed and autofluorescence signals were 465 to 485 nm, 500 to 530 nm, 525 to 550nm, 600 to 630 and 620 to 720 nm respectively, and emitted fluorescence was false-colored in magenta (CFP), green (GFP or YFP) and red (DsRed and/or wall autofluorescence). The images shown are single confocal sections, maximal projections of selected planes of a z-stack or 3D-reconstructions of confocal image stacks. Images were acquired and projected using Leica confocal software and processed using Leica, ImageJ (http://imagej.nih.gov/ij/) or Volocity version 6.0.1 (Perkin-Elmer) softwares.

β-galactosidase assay

Histochemical staining for β-galactosidase activity after inoculation with *S. meliloti* strain *Sm* 2011-*lacZ* was performed 3 d post inoculation using X-gal as substrate (Boivin et al., 1990). Data in Fig. 3A-C are representative of results obtained in 10 A17 and 10 *Mtnin-1* plants.

Supplemental Material

Supplemental Figure S1. Radial expansion of the infection chamber prior to thread initiation.

Supplemental Figure S2. Infection chamber development and associated rhizobial multiplication are blocked in curled root hairs of the *Mtnin* mutant.

Supplemental Figure S3. Before infection chamber closure, the localization of GFP-VAMP721e in *Mtnin*-1 root hairs is similar to that in a wild-type plant.

Supplemental Movie 1. Animation illustrating the 2-step model for rhizobial root hair infection initiation.

Acknowledgements

We are grateful to P. Smit (Wageningen, The Netherlands) for providing the *S. meliloti* 2011 strains expressing cCFP or GFP, to Tatiana Vernié and Giles Oldroyd (John Innes Center, UK) for providing the *Mtnin-1* seeds and to Alain Jauneau and colleagues from the FR 3450 imagery facility for their assistance with confocal microscopy.

Literature cited

Ardourel M, Demont N, Debelle FD, Maillet F, Debilly F, Prome JC, Denarie J, Truchet G (1994) *Rhizobium meliloti* lipochitooligosaccharide nodulation factors - Different structural requirements for bacterial entry into target root hair cells and induction of plant symbiotic developmental responses. Plant Cell **6:** 1357-1374

Bapaume L, Reinhardt D (2012) How membranes shape plant symbioses: signaling and transport in nodulation and arbuscular mycorrhiza. Front Plant Sci **3:** 223

Boisson-Dernier A, Andriankaja A, Chabaud M, Niebel A, Journet EP, Barker DG, de Carvalho-Niebel F (2005) *MtENOD11* gene activation during rhizobial infection and mycorrhizal arbuscule development requires a common AT-rich-containing regulatory sequence. Mol Plant Microbe Interact **18:** 1269-1276

Boisson-Dernier A, Chabaud M, Garcia F, Bécard G, Rosenberg C, Barker DG (2001) *Agrobacterium rhizogenes*-transformed roots of *Medicago truncatula* for the study of nitrogen-fixing and endomycorrhizal symbiotic associations. Mol Plant Microbe Interact **14:** 695-700

Boivin C, Camut S, Malpica CA, Truchet G, Rosenberg C (1990) *Rbizobium meliloti* genes encoding catabolism of trigonelline are induced under symbiotic conditions. Plant Cell **2:** 1157-1170

Borisov AY, Madsen LH, Tsyganov VE, Umehara Y, Voroshilova VA, Batagov AO, Sandal N, Mortensen A, Schauser L, Ellis N, Tikhonovich IA, Stougaard J (2003) The *Sym35* gene required for root nodule development in pea is an ortholog of *Nin* from *Lotus japonicus*. Plant Physiol **131:** 1009-1017

Brewin NJ (1991) Development of the legume root nodule. Ann Rev Cell Biol **7:** 191-226

Brewin NJ (2004) Plant cell wall remodelling in the rhizobium-legume symbiosis. Crit Rev Plant Sci **23:** 293-316

Callaham DA, Torrey JG (1981) The structural basis for infection of root hairs of *Trifolium repens* by *Rhizobium*. Can J Bot **59:** 1647-1664

Capoen W, Sun J, Wysham D, Otegui MS, Venkateshwaran M, Hirsch S, Miwa H, Downie JA, Morris RJ, Ane JM, Oldroyd GED (2011) Nuclear membranes control symbiotic calcium signaling of legumes. Proc Natl Acad Sci USA **108:** 14348-14353

Catoira R, Timmers ACJ, Maillet F, Galera C, Penmetsa RV, Cook D, Denarie J, Gough C (2001) The *HCL* gene of *Medicago truncatula* controls *Rhizobium*-induced root hair curling. Development **128:** 1507-1518

Cerri MR, Frances L, Laloum T, Auriac MC, Niebel A, Oldroyd GED, Barker DG, Fournier J, de Carvalho-Niebel F (2012) *Medicago truncatula* ERN transcription factors: regulatory interplay with NSP1/NSP2 GRAS factors and expression dynamics throughout rhizobial iInfection. Plant Physiol **160:** 2155-2172

Charron D, Pingret JL, Chabaud M, Journet EP, Barker DG (2004) Pharmacological evidence that multiple phospholipid signaling pathways link *Rhizobium* nodulation factor perception in *Medicago truncatula* root hairs to intracellular responses, including Ca^{2+} spiking and specific *ENOD* gene expression. Plant Physiol **136:** 3582-3593

Dart PJ (1974) The infection process. *In* A Quispel, ed, The biology of nitrogen fixation. North-Holland Publishing Co., Amsterdam, pp 381-429

Downie JA (2010) The roles of extracellular proteins, polysaccharides and signals in the interactions of rhizobia with legume roots. FEMS Microbiol Rev **34:** 150-170

Ehrhardt DW, Wais R, Long SR (1996) Calcium spiking in plant root hairs responding to *Rhizobium* nodulation signals. Cell **85:** 673-681

Esseling JJ, Lhuissier FGP, Emons AMC (2003) Nod factor-induced root hair curling: Continuous polar growth towards the point of nod factor application. Plant Physiol **132:** 1982-1988

Fournier J, Timmers ACJ, Sieberer BJ, Jauneau A, Chabaud M, Barker DG (2008) Mechanism of infection thread elongation in root hairs of *Medicago truncatula* and dynamic interplay with associated rhizobial colonization. Plant Physiol **148:** 1985-1995

Fåhraeus G (1957) The infection of clover root hairs by nodule bacteria studied by a simple glass slide technique. J Gen Microbiol **16:** 374-381

Gage DJ (2002) Analysis of infection thread development using Gfp- and DsRed-expressing *Sinorhizobium meliloti*. J Bacteriol **184:** 7042-7046

Gage DJ (2004) Infection and invasion of roots by symbiotic, nitrogen-fixing rhizobia during nodulation of temperate legumes. Microbiol Mol Biol Rev **68:** 280-300

Gage DJ, Bobo T, Long SR (1996) Use of green fluorescent protein to visualize the early events of symbiosis between *Rhizobium meliloti* and alfalfa (*Medicago sativa*). J Bacteriol **178:** 7159-7166

Genre A, Chabaud M, Faccio A, Barker DG, Bonfante P (2008) Prepenetration apparatus assembly precedes and predicts the colonization patterns of arbuscular mycorrhizal fungi within the root cortex of both *Medicago truncatula* and *Daucus carota*. Plant Cell **20:** 1407-1420

Genre A, Chabaud M, Timmers T, Bonfante P, Barker DG (2005) Arbuscular mycorrhizal fungi elicit a novel intracellular apparatus in *Medicago truncatula* root epidermal cells before infection. Plant Cell **17:** 3489-3499

Genre A, Ivanov S, Fendrych M, Faccio A, Zarsky V, Bisseling T, Bonfante P (2012) Multiple exocytotic markers accumulate at the sites of perifungal membrane biogenesis in arbuscular mycorrhizas. Plant Cell Physiol **53:** 244-255

Geurts R, Fedorova E, Bisseling T (2005) Nod factor signaling genes and their function in the early stages of *Rhizobium* infection. Curr Opin Plant Biol **8:** 346-352

Goormachtig S, Capoen W, Holsters M (2004) *Rhizobium* infection: lessons from the versatile nodulation behaviour of water-tolerant legumes. Trends Plant Sci **9:** 518-522

Guan D, Stacey N, Liu CW, Wen JQ, Mysore KS, Torres-Jerez I, Vernie T, Tadege M, Zhou CN, Wang ZY, Udvardi MK, Oldroyd GED, Murray JD (2013) Rhizobial infection is associated with the development of peripheral vasculature in nodules of *Medicago truncatula*. Plant Physiol **162:** 107-115

Ivanov S, Fedorova EE, Limpens E, De Mita S, Genre A, Bonfante P, Bisseling T (2012) *Rhizobium*-legume symbiosis shares an exocytotic pathway required for arbuscule formation. Proc Natl Acad Sci USA **109:** 8316-8321

Journet EP, El-Gachtouli N, Vernoud V, de Billy F, Pichon M, Dedieu A, Arnould C, Morandi D, Barker DG, Gianinazzi-Pearson V (2001) *Medicago truncatula ENOD11*: A novel RPRP-encoding early nodulin gene expressed during mycorrhization in arbuscule-containing cells. Mol Plant-Microbe Interact **14:** 737-748

Kijne JW (1992) The Rhizobium infection process. *In* G Stacey, RH Burris, HJ Evans, eds, Biological Nitrogen Fixation. Chapman and Hall, New York, pp 349-398

Kistner C, Parniske M (2002) Evolution of signal transduction in intracellular symbiosis. Trends Plant Sci **7:** 511-518

Kuppusamy KT, Endre G, Prabhu R, Penmetsa RV, Veereshlingam H, Cook DR, Dickstein R, VandenBosch KA (2004) *LIN*, a Medicago truncatula gene required for nodule differentiation and persistence of rhizobial infections. Plant Physiol **136:** 3682-3691

Limpens E, Franken C, Smit P, Willemse J, Bisseling T, Geurts R (2003) LysM domain receptor kinases regulating rhizobial Nod factor-induced infection. Science **302:** 630-633

Limpens E, Ivanov S, van Esse W, Voets G, Fedorova E, Bisseling T (2009) *Medicago* N-2-fixing symbiosomes acquire the endocytic identity marker Rab7 but delay the acquisition of vacuolar identity. Plant Cell **21:** 2811-2828

Markmann K, Parniske M (2009) Evolution of root endosymbiosis with bacteria: how novel are nodules? Trends Plant Sci **14:** 77-86

Marsh JF, Rakocevic A, Mitra RM, Brocard L, Sun J, Eschstruth A, Long SR, Schultze M, Ratet P, Oldroyd GE (2007) *Medicago truncatula NIN* is essential for rhizobial-independent nodule organogenesis induced by autoactive calcium/calmodulin-dependent protein kinase. Plant Physiol **144:** 324-335

Murray JD (2011) Invasion by Invitation: Rhizobial Infection in Legumes. Mol Plant-Microbe Interact **24:** 631-639

Oldroyd GED (2013) Speak, friend, and enter: signalling systems that promote beneficial symbiotic associations in plants. Nat Rev Microbiol **11:** 252-263

Oldroyd GED, Downie JA (2006) Nuclear calcium changes at the core of symbiosis signalling. Curr Opin Plant Biol **9:** 351-357

Oldroyd GED, Murray JD, Poole PS, Downie JA (2011) The rules of engagement in the legume-rhizobial symbiosis. Ann Rev Genet **45**: 119-144

Parniske M (2008) Arbuscular mycorrhiza: the mother of plant root endosymbioses. Nat Rev Microbiol **6:** 763-775

Pichon M, Journet EP, Dedieu A, de Billy F, Truchet G, Barker DG (1992) *Rhizobium meliloti* elicits transient expression of the early nodulin gene *ENOD12* in the differentiating root epidermis of transgenic alfalfa. Plant Cell **4:** 1199-1211

Quandt HJ, Puhler A, Broer I (1993) Transgenic root nodules of *Vicia hirsuta* - a fast and efficient system for the study of gene expression in indeterminate-type nodules. Mol Plant-Microbe Interact **6:** 699-706

Rich MK, Schorderet M, Reinhardt D (2014) The role of the cell wall compartment in mutualistic symbioses of plants. Front Plant Sci **5:** 238

Robledo M, Jimenez-Zurdo JI, Velazquez E, Trujillo ME, Zurdo-Pineiro JL, Ramirez-Bahena MH, Ramos B, Diaz-Minguez JM, Dazzo F, Martinez-Molina E, Mateos PF (2008) *Rhizobium* cellulase CelC2 is essential for primary symbiotic infection of legume host roots. Proc Natl Acad Sci USA **105:** 7064-7069

Schauser L, Roussis A, Stiller J, Stougaard J (1999) A plant regulator controlling development of symbiotic root nodules. Nature **402:** 191-195

Scheres B, Van De Wiel C, Zalensky A, Horvath B, Spaink H, Vaneck H, Zwartkruis F, Wolters AM, Gloudemans T, Vankammen A, Bisseling T (1990) The *ENOD12* gene product is involved in the infection process during the pea-*Rhizobium* interaction. Cell **60:** 281-294

Schnabel E, Journet EP, de Carvalho-Niebel F, Duc G, Frugoli J (2005) The *Medicago truncatula SUNN* gene encodes a CLV1-like leucine-rich repeat receptor kinase that regulates nodule number and root length. Plant Mol Biol **58:** 809-822

Sieberer BJ, Chabaud M, Fournier J, Timmers AC, Barker DG (2012) A switch in Ca^{2+} spiking signature is concomitant with endosymbiotic microbe entry into cortical root cells of *Medicago truncatula*. Plant J **69:** 822-830

Sieberer BJ, Chabaud M, Timmers AC, Monin A, Fournier J, Barker DG (2009) A Nuclear-targeted cameleon demonstrates intranuclear Ca^{2+} spiking in *Medicago truncatula* root hairs in response to rhizobial nodulation factors. Plant Physiol **151:** 1197-1206

Sieberer BJ, Fournier J, Timmers ACJ, Chabaud M, Barker DG (2015) Nuclear Ca^{2+} signaling reveals active bacterial-host signaling throughout rhizobial infection in root hairs of *Medicago truncatula*. *In* FJ de Bruijn, ed, Biologial Nitrogen Fixation. Wiley/Blackwell, Hoboken, NJ, USA *in press*

Singh S, Parniske M (2012) Activation of calcium- and calmodulin-dependent protein kinase (CCaMK), the central regulator of plant root endosymbiosis. Curr Opin Plant Biol **15:** 444-453

Smit P, Limpens E, Geurts R, Fedorova E, Dolgikh E, Gough C, Bisseling T (2007) Medicago LYK3, an entry receptor in rhizobial nodulation factor signaling. Plant Physiol **145:** 183-191

Smit P, Raedts J, Portyanko V, Debelle F, Gough C, Bisseling T, Geurts R (2005) NSP1 of the GRAS protein family is essential for rhizobial Nod factor-induced transcription. Science **308:** 1789-1791

Turgeon BG, Bauer WD (1985) Ultrastructure of infection thread development during the infection of soybean by *Rhizobium japonicum*. Planta **163:** 328-349

Wais RJ, Wells DH, Long SR (2002) Analysis of differences between *Sinorhizobium meliloti* 1021 and 2011 strains using the host calcium spiking response. Mol Plant-Microbe Interact **15:** 1245-1252

Xie F, Murray JD, Kim J, Heckmann AB, Edwards A, Oldroyd GED, Downie A (2012) Legume pectate lyase required for root infection by rhizobia. Proc Natl Acad Sci USA **109:** 633-638

Yano K, Yoshida S, Muller J, Singh S, Banba M, Vickers K, Markmann K, White C, Schuller B, Sato S, Asamizu E, Tabata S, Murooka Y, Perry J, Wang TL, Kawaguchi M, Imaizumi-Anraku H, Hayashi M, Parniske M (2008) CYCLOPS, a mediator of symbiotic intracellular accommodation. Proc Natl Acad Sci USA **105:** 20540-20545

Figure legends

Figure 1. Infection thread initiation does not immediately follow rhizobial entrapment within the curled root hair. Bright field (left panel) and the corresponding confocal (right panel) images of a *M. truncatula* RH at different times following tip curling around GFP-labelled *S. meliloti* 2011. In the bright field images the location of the nucleus (n) is indicated, as well as the position of the RH tip (arrowhead, A-C). In the fluorescence images the region of the cell wall adjacent to the infection chamber where auto-fluorescent material accumulates is indicated (double arrowhead, C-E). Note that the IT walls (E) are devoid of auto-fluorescent material in contrast to the rest of the RH wall. Confocal images of GFP fluorescence (single optical sections across the infection chamber) were superposed either with the laser transmission images (left panel) or with the cell wall auto-fluorescence (right panel). cb: cytoplasmic bridge. Bars = 10 µm.

Figure 2. GFP-MtVAMP721e identifies exocytotic activity surrounding the infection chamber in curled root hairs. A to C, The intracellular localization of the GFP-MtVAMP721e fusion (green) in *M. truncatula* RHs was imaged over a 7 h period in both a curled hair and an adjacent tip-growing hair after inoculation with cCFP-labeled *S. meliloti* (magenta). A, The GFP-VAMP721e fusion protein fluorescence surrounds the enclosed bacteria (open arrowhead) within the infection chamber of the curled RH (left hair, arrow) whereas GFP fluorescence localizes predominantly to the tip of the growing RH (hair on the right, solid arrowhead). B and C, Throughout the 7 h monitoring period the GFP fluorescence localizes to the periphery of the infection chamber, which undergoes progressive radial expansion within the curled RH. D to F, Identical RH as in A-C, showing in more detail that the cCFP-labeled rhizobia within the infection chamber (open arrowhead) have multiplied concomitantly with chamber expansion. The dashed lines indicate the RH contours. G to J, GFP-MtVAMP721e localization in RHs that are just completing curling. The completion of RH curling around an attached Rhizobium (open arrowhead) occurs during the 1h30 observation period, and is associated with the rapid loss (dashed arrow in H) of the tip-localized GFP fluorescence (arrow in G). I and J, In a second RH, two different stages are identified by GFP-MtVAMP721e localization (arrows). I, As in (G), tip-localized GFP fluorescence indicates that the RH is still curling. J, 3h30 later, curling has terminated and GFP is now found predominantly around the closed infection chamber (open arrowhead), whereas the RH tip fluorescence has been lost (not in focal plane)**.** Confocal images are based on single optical sections across the infection chamber for A-C, z-axis projections of 7 serial optical sections encompassing the entire rhizobial microcolony for D-F, three-dimensional images reconstructed from confocal z-stacks (22 serial optical sections) for G-H, z-axis projection of 5 serial optical sections encompassing the RH tip and attached rhizobia for I and z-axis

projection of 2 serial optical sections across the infection chamber for J. n: nucleus. Bars = 10 µm.

Figure 3. In the infection-defective *Mtnin* mutant entrapment of rhizobia within the infection chamber is not followed by targeted exocytosis nor bacterial multiplication. A to C, Rhizobial microcolony development is strongly reduced in *Mtnin-1* compared to the wild type (WT), as indicated by the level of β-galactosidase activity of *S. meliloti* (*hemA-LacZ*) colonies (arrows) entrapped within curled RHs of wild type A17 (A) or *Mtnin-1* (B, C) plants. D to F, The GFP-VAMP721e fusion protein does not accumulate at the periphery of the infection chamber (arrowhead) in *Mtnin-1* plants expressing the exocytosis reporter, although cCFP-labeled *S. meliloti* (magenta) are present in the chamber. Note that, as for the wild type, background GFP-VAMP721e fluorescence was detected in both the cytoplasm and cytoplasmic bodies. G to I, Consistent with A-C, the rhizobial microcolony in the *nin* mutant does not visibly enlarge over the observation period compared to wild type (see Fig. 2). The dashed lines indicate the RH contours. n, nucleus. Bars = 10 µm.

Figure 4. YFP-MtENOD11 accumulates within the rhizobial infection chamber preceding infection thread initiation. Early RH infection sites were imaged in *M. truncatula* roots expressing a YFP-tagged ENOD11 fusion (green) following inoculation with cCFP-expressing *S. meliloti* (magenta). A and B, Prior to IT formation, the YFP-MtENOD11 fluorescence (arrow, A) is mainly associated with the infection chamber surrounding the enclosed rhizobia (open arrowhead, A-B). The double arrowhead indicates the auto-fluorescent wall domain (in red) adjacent to the infection chamber contrasting with the absence of autofluorescence associated to the infection chamber (dashed arrow in B). C and D, An IT is initiating from an infection chamber that has formed after rhizobia have become entrapped between two touching RHs (RH1 and RH2). YFP-MtENOD11 accumulation is associated with the site of initial rhizobial enclosure between touching walls (arrow), the protruding infection chamber formed in RH2 (open arrowhead), as well as the tip of the initiating IT (bracket). Confocal images are z-axis projections of 5 (A-B) or 13 (C,D) serial optical sections. A, C: overlays of cCFP (magenta), YFP (green) and auto-fluorescence (red); and B, D: overlays of cCFP and auto-fluorescence. The dashed lines in D indicate the contours of the RH cells. Bars = 10 µm.

Figure 5. Infection chamber remodeling paves the way for polar infection thread initiation in *M. truncatula* root hairs. The localization of the exocytosis reporter and the MtENOD11 protein during RH curling, infection chamber remodeling and IT initiation are schematically represented. A to C, During RH curling, the GFP-VAMP721e-labeled exocytosis site at the growing RH tip (A-B) is lost once RH curling is completed (C). At this stage, the infection chamber generally encloses a single *Rhizobium* cell. D to F, Remodeling of the infection chamber starts during the following hours before significant rhizobial multiplication has

occurred (D) and leads to enlargement and differentiation of this new compartment accompanied by rhizobial multiplication (E) prior to tubular IT initiation (F). Note that the *Mtnin-1* mutant fails to progress from stage C to stage D. Color code: Rhizobia, pink; GFP-MtVAMP721e, green; YFP-MtENOD11, yellow.

Supplemental Figure S1. Radial expansion of the infection chamber prior to thread initiation. During the lengthy 10-20 h period preceding IT initiation, the infection chamber (arrow) progressively enlarges and becomes clearly distinguishable from the surrounding cytoplasm. This is likely to be the result of exocytotic activity and wall remodeling. The RH tip is the same as that shown in Fig. 1. n, nucleus. Bar = 10 µm.

Supplemental Figure S2. Infection chamber development and associated rhizobial multiplication are blocked in curled root hairs of the *Mtnin* mutant. Images of the identical RH extremity shown in Fig. 3 (D to I) taken at later time-points as indicated show that neither infection chamber labeling with GFP-VAMP721e nor multiplication of the enclosed cCFP-labeled rhizobia (arrowhead) have significantly changed, indicating that both processes are blocked rather than simply delayed in the *Mtnin-1* mutant. The dashed lines indicate the RH contours. Bar = 10 µm.

Supplemental Figure S3. Before infection chamber closure, the localization of GFP-VAMP721e in *Mtnin*-1 root hairs is similar to that in a wild-type plant. In *Mtnin*-1 roots expressing the GFP-MtVAMP721e fusion (green), the main GFP fluorescence in a growing, non-curled root hair (A-B) or a curling root hair (C,D) is associated to the vesicle-rich region at the growing tip (solid arrowhead) similar to wild-type growing root hairs (see Figure 2A) and wild-type curling root hairs (see Fig.2G and I). Bar = 10 µm.

Supplemental Movie 1. Animation illustrating the 2-step model for rhizobial root hair infection initiation. The first 15 s of the animation illustrate the processes of RH tip growth, *Rhizobium* attachment and resulting re-orientation of RH tip growth till rhizobial entrapment. The second half of the animation represents a virtual section across the curled RH and is broadly based on the scheme shown in Figure 5D-F with the exocytosis activity represented by the accumulation of vesicles (dark blue) initially at the periphery of the radially growing infection chamber and then subsequently at the apically growing tip of the IT. Note also that, according to results presented in an earlier publication (Fournier et al., 2008), IT tip growth always precedes rhizobial colonization and that this progressive colonization of the IT occurs both by division and physical movement (sliding) of the bacteria. Other color coding:

Rhizobia, red; Plant cytoplasm, light blue; Nucleus, green; Infection chamber/IT lumen, yellow; Vacuole, grey.

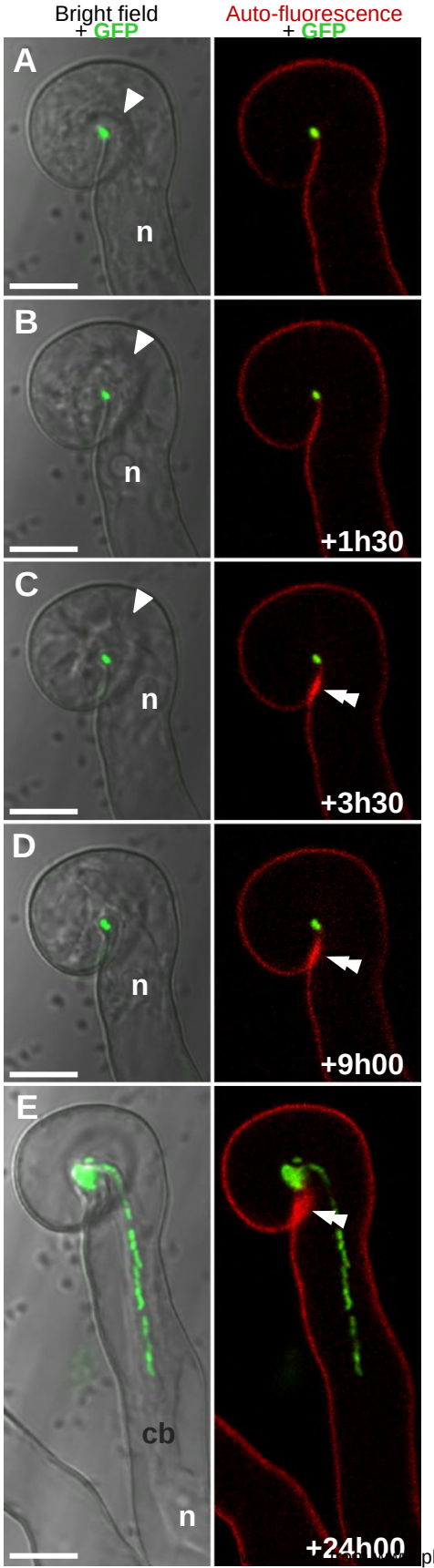

Figure 1. Infection thread initiation does not immediately follow rhizobial entrapment within the curled root hair. Bright field (left panel) and the corresponding confocal (right panel) images of a *M. truncatula* RH at different times following tip curling around GFP-labelled *S. meliloti* 2011. In the bright field images the location of the nucleus (n) is indicated, as well as the position of the RH tip (arrowhead, A-C). In the fluorescence images the region of the cell wall adjacent to the infection chamber where auto-fluorescent material accumulates is indicated (double arrowhead, C-E). Note that the IT walls (E) are devoid of auto-fluorescent material in contrast to the rest of the RH wall. Confocal images of GFP fluorescence (single optical sections across the infection chamber) were superposed either with the laser transmission images (left panel) or with the cell wall auto-fluorescence (right panel). cb: cytoplasmic bridge. Bars = 10 µm.

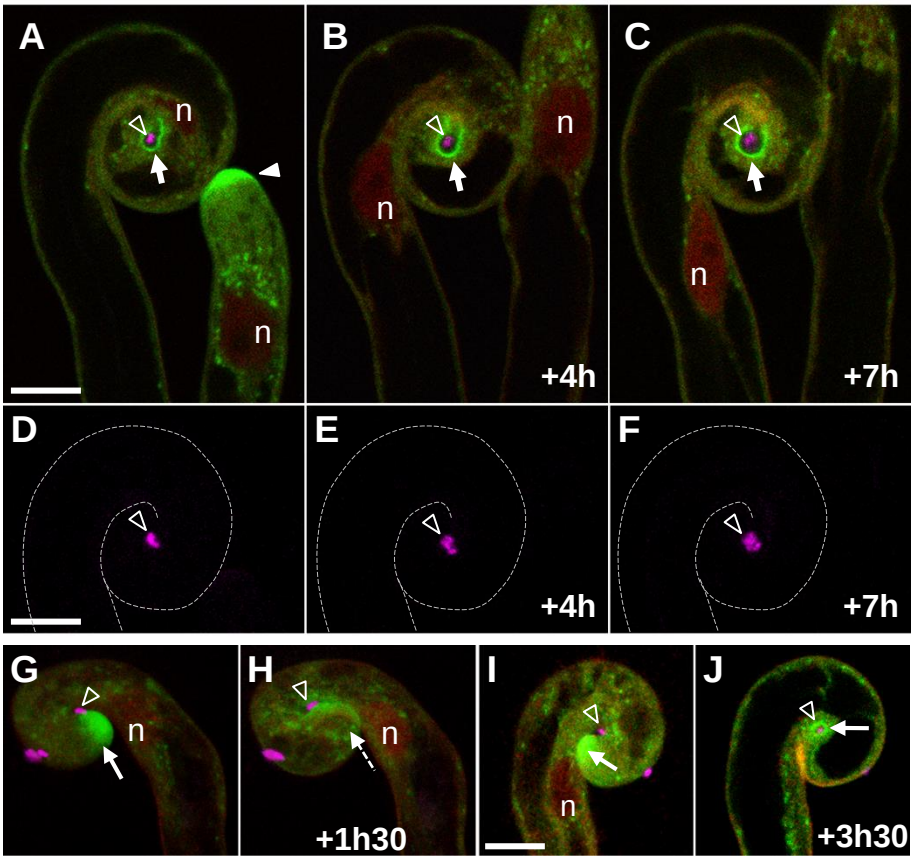

Figure 2. GFP-MtVAMP721e identifies exocytotic activity surrounding the infection chamber in curled root hairs. A to C, The intracellular localization of the GFP-MtVAMP721e fusion (green) in *M. truncatula* RHs was imaged over a 7 h period in both a curled hair and an adjacent tip-growing hair after inoculation with cCFP-labeled *S. meliloti* (magenta). A, The GFP-VAMP721e fusion protein fluorescence surrounds the enclosed bacteria (open arrowhead) within the infection chamber of the curled RH (left hair, arrow) whereas GFP fluorescence localizes predominantly to the tip of the growing RH (hair on the right, solid arrowhead). B and C, Throughout the 7 h monitoring period the GFP fluorescence localizes to the periphery of the infection chamber, which undergoes progressive radial expansion within the curled RH. D to F, Identical RH as in A-C, showing in more detail that the cCFP-labeled rhizobia within the infection chamber (open arrowhead) have multiplied concomitantly with chamber expansion. The dashed lines indicate the RH contours. G to J, GFP-MtVAMP721e localization in RHs that are just completing curling. G and H, The completion of RH curling around an attached Rhizobium (open arrowhead) occurs during the 1h30 observation period, and is associated with the rapid loss (dashed arrow in H) of the tip-localized GFP fluorescence (arrow in G). I and J, In a second RH, two different stages are identified by GFP-MtVAMP721e localization (arrows). I, As in (G), tip-localized GFP fluorescence indicates that the RH is still curling. J, 3h30 later, curling has terminated and GFP is now found predominantly around the closed infection chamber (open arrowhead), whereas the RH tip fluorescence has been lost (not in focal plane)**.** Confocal images are based on single optical sections across the infection chamber for A-C, z-axis projections of 7 serial optical sections encompassing the entire rhizobial microcolony for D-F, three-dimensional images reconstructed from confocal z-stacks (22 serial optical sections) for G-H, z-axis projection of 5 serial optical sections encompassing the RH tip and attached rhizobia for I and z-axis projection of 2 serial optical sections across the infection chamber for J. n, nucleus. Bars = 10 µm.

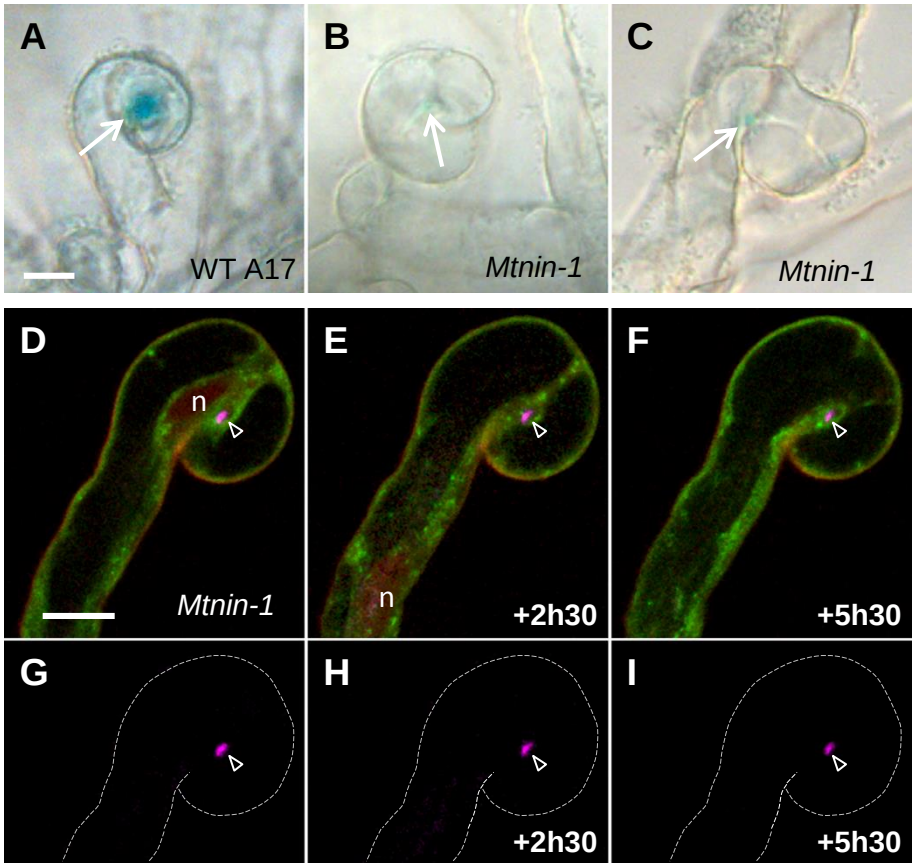

Figure 3. In the infection-defective *Mtnin* mutant entrapment of rhizobia within the infection chamber is not followed by targeted exocytosis nor bacterial multiplication. A to C, Rhizobial microcolony development is strongly reduced in *Mtnin-1* compared to the wild type (WT), as indicated by the level of β-galactosidase activity of *S. meliloti* (*hemA-LacZ*) colonies (arrows) entrapped within curled RHs of wild type A17 (A) or *Mtnin-1* (B, C) plants. D to F, The GFP-VAMP721e fusion protein does not accumulate at the periphery of the infection chamber (arrowhead) in *Mtnin-1* plants expressing the exocytosis reporter, although cCFP-labeled *S. meliloti* (magenta) are present in the chamber. Note that, as for the wild type, background GFP-VAMP721e fluorescence was detected in both the cytoplasm and cytoplasmic bodies. G to I, Consistent with A-C, the rhizobial microcolony in the *nin* mutant does not visibly enlarge over the observation period compared to wild type (see Fig. 2). The dashed lines indicate the RH contours. n, nucleus. Bars = 10 µm.

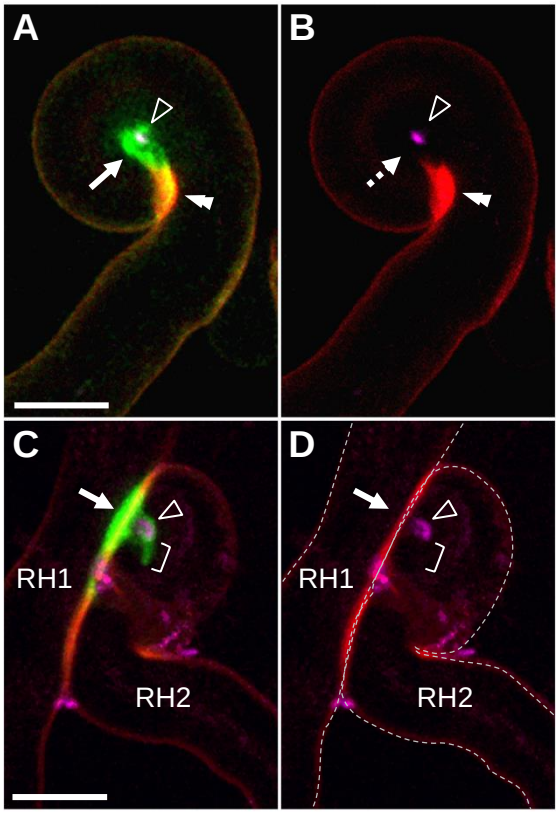

Figure 4. YFP-MtENOD11 accumulates within the rhizobial infection chamber preceding infection thread initiation. Early RH infection sites were imaged in *M. truncatula* roots expressing a YFP-tagged ENOD11 fusion (green) following inoculation with cCFP-expressing *S. meliloti* (magenta). A and B, Prior to IT formation, the YFP-MtENOD11 fluorescence (arrow, A) is mainly associated with the infection chamber surrounding the enclosed rhizobia (open arrowhead, A-B). The double arrowhead indicates the auto-fluorescent wall domain (in red) adjacent to the infection chamber contrasting with the absence of autofluorescence associated to the infection chamber (dashed arrow in B). C and D, An IT is initiating from an infection chamber that has formed after rhizobia have become entrapped between two touching RHs (RH1 and RH2). YFP-MtENOD11 accumulation is associated with the site of initial rhizobial enclosure between touching walls (arrow), the protruding infection chamber formed in RH2 (open arrowhead), as well as the tip of the initiating IT (bracket). Confocal images are z-axis projections of 5 (A-B) or 13 (C,D) serial optical sections. A, C: overlays of cCFP (magenta), YFP (green) and auto-fluorescence (red); and B, D: overlays of cCFP and auto-fluorescence. The dashed lines in D indicate the contours of the RH cells. Bars = 10 µm.

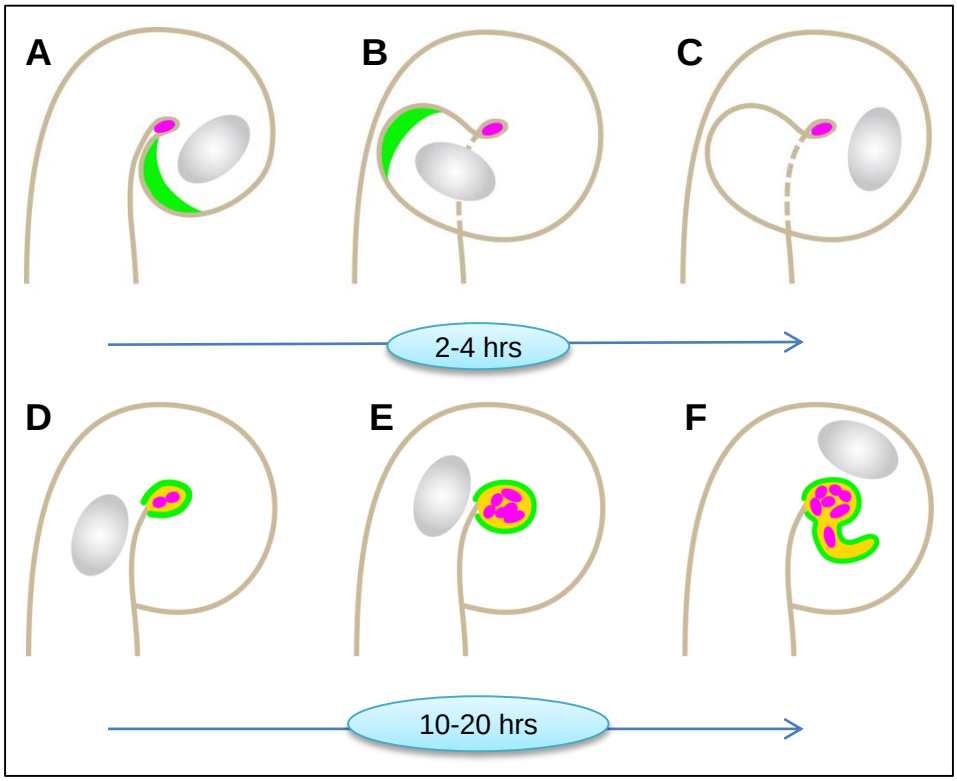

Figure 5. Infection chamber remodeling paves the way for polar infection thread initiation in *M. truncatula* root hairs. The localization of the exocytosis reporter and the MtENOD11 protein during RH curling, infection chamber remodeling and IT initiation are schematically represented. A to C, During RH curling, the GFP-VAMP721e-labeled exocytosis site at the growing RH tip (A-B) is lost once RH curling is completed (C). At this stage, the infection chamber generally encloses a single *Rhizobium* cell. D to F, Remodeling of the infection chamber starts during the following hours before significant rhizobial multiplication has occurred (D) and leads to enlargement and differentiation of this new compartment accompanied by rhizobial multiplication (E) prior to tubular IT initiation (F). Note that the *Mtnin-1* mutant fails to progress from stage C to stage D. Color code: Rhizobia, pink; GFP-MtVAMP721e, green; YFP-MtENOD11, yellow.